

AD-A191 635

# STUDIES OF OPTICAL MATRIX MULTIPLICATION AND RECONFIGURABLE OPTICAL INTERCONNECT CONCEPTS

ANNUAL TECHNICAL REPORT NO. 1 FOR THE PERIOD  
November 1, 1986 through October 31, 1987

CONTRACT NO. F49620-87-C-0015

Prepared for

Directorate of Electronic and Material Sciences  
ATTN: AFOSR/NE, Dr. C. Giles  
Building 410  
Bolling AFB, DC 20332-6448

Pochi Yeh  
Principal Investigator

JANUARY 1988

DTIC  
ELECTE  
FEB 29 1988  
S H D

Approved for public release; distribution unlimited

The views and conclusions contained in this document are those of the authors and should not be interpreted as necessarily representing the official policies, either expressed or implied, of the Defense Advanced Research Projects Agency or the U.S. Government.



Rockwell International  
Science Center

UNCLASSIFIED

SECURITY CLASSIFICATION OF THIS PAGE

## REPORT DOCUMENTATION PAGE

FORM APPROVED  
OMB no. 0704-0188

1a. REPORT SECURITY CLASSIFICATION <b>UNCLASSIFIED</b>			1b. RESTRICTIVE MARKINGS														
2a. SECURITY CLASSIFICATION AUTHORITY			3. DISTRIBUTION/AVAILABILITY OF REPORT  <b>Approved for public release; distribution unlimited</b>														
2b. CLASSIFICATION/DOWNGRADING SCHEDULE																	
4. PERFORMING ORGANIZATION REPORT NUMBER(S) <b>SC5502.AR</b>			5. MONITORING ORGANIZATION REPORT NUMBER(S)  <b>AFOSR-TR- 88-0094</b>														
6a. NAME OF PERFORMING ORGANIZATION <b>ROCKWELL INTERNATIONAL Science Center</b>		6b. OFFICE SYMBOL (If Applicable)		7a. NAME OF MONITORING ORGANIZATION  <b>AFOSR/NE BLDG 410 BOLLING AFB, DC 20332-6448</b>													
6c. ADDRESS (City, State, and ZIP Code) <b>1049 Camino Dos Rios Thousand Oaks, CA 91360</b>																	
8a. NAME OF FUNDING/SPONSORING ORGANIZATION <b>Directorate of Electronic and Material Sciences</b>		8b. OFFICE SYMBOL (If Applicable)		9. PROCUREMENT INSTRUMENT IDENTIFICATION NUMBER  <b>CONTRACT NO. F49620-87-C-0015</b>													
8c. ADDRESS (City, State and ZIP Code) <b>Building 410 Bolling AFB, DC 20332-6448</b>				10. SOURCE OF FUNDING NOS. <table border="1"> <tr> <td>PROGRAM ELEMENT NO. <b>61102F</b></td> <td>PROJECT NO. <b>Arpa Order No. 5884</b></td> <td>TASK NO.</td> <td>WORK UNIT ACCESSION NO.</td> </tr> </table>		PROGRAM ELEMENT NO. <b>61102F</b>	PROJECT NO. <b>Arpa Order No. 5884</b>	TASK NO.	WORK UNIT ACCESSION NO.								
PROGRAM ELEMENT NO. <b>61102F</b>	PROJECT NO. <b>Arpa Order No. 5884</b>	TASK NO.	WORK UNIT ACCESSION NO.														
11. TITLE (Include Security Classification) <b>STUDIES OF OPTICAL MATRIX MULTIPLICATION AND RECONFIGURABLE OPTICAL INTERCONNECT CONCEPTS</b>																	
12. PERSONAL AUTHOR(S) <b>Yeh, Pochi; Chiou, A.E.T.</b>																	
13a. TYPE OF REPORT <b>Annual Technical Report No. 1</b>		13b. TIME COVERED FROM <b>11/01/86</b> TO <b>10/31/87</b>		14. DATE OF REPORT (Year, Month, Day) <b>1988, JANUARY</b>													
15. PAGE COUNT <b>37</b>																	
16. SUPPLEMENTARY NOTATION <b>The views and conclusions contained in this document are those of the authors and should not be interpreted as necessarily representing the official policies either expressed or implied, of the Defense Advanced Research Projects Agency or the U.S. Government.</b>																	
17. COSATI CODES <table border="1"> <tr> <th>FIELD</th> <th>GROUP</th> <th>SUB-GROUP</th> </tr> <tr><td></td><td></td><td></td></tr> <tr><td></td><td></td><td></td></tr> <tr><td></td><td></td><td></td></tr> </table>			FIELD	GROUP	SUB-GROUP										18. SUBJECT TERMS (Continue on reverse if necessary and identify by block number)		
FIELD	GROUP	SUB-GROUP															
19. ABSTRACT (Continue on reverse if necessary and identify by block number)  <b>In the first year of the program, we studied a number of concepts on matrix multiplication and reconfigurable optical interconnection using photorefractive materials such as BaTiO<sub>3</sub>. We have also conceived several new concepts in the same area. The results are documented in three technical paper/presentations and four patent disclosures.</b>																	
20. DISTRIBUTION/AVAILABILITY OF ABSTRACT UNCLASSIFIED/UNLIMITED <input type="checkbox"/> SAME AS RPT. <input checked="" type="checkbox"/> DTIC USERS <input type="checkbox"/>			21. ABSTRACT SECURITY CLASSIFICATION <b>UNCLASSIFIED</b>														
22a. NAME OF RESPONSIBLE INDIVIDUAL <b>Giles</b>			22b. TELEPHONE NUMBER (Include Area Code) <b>(202) 767-4933</b>		22c. OFFICE SYMBOL <b>NE</b>												

DD FORM 1473, JUN 86

Previous editions are of solete.

UNCLASSIFIED

SECURITY CLASSIFICATION OF THIS PAGE



SC5502.AR

## TABLE OF CONTENTS

	<u>Page</u>
1.0 SUMMARY .....	1
1.1 Contract Description .....	1
1.2 Scientific Problem .....	1
1.3 Progress .....	1
1.4 Publications and Presentations .....	2
1.5 Patent Disclosures .....	2
2.0 TECHNICAL DISCUSSION .....	3
2.1 Matrix-Matrix Multiplication .....	4
2.2 Matrix-Vector Multiplication .....	7
2.3 Reconfigurable Optical Interconnect .....	7
3.0 PROGRESS .....	11
3.1 Matrix-Vector Multiplication .....	11
3.2 Matrix-Matrix Multiplication via Color Multiplexing .....	12
3.3 Matrix-Matrix Multiplication using Spatial Convolution .....	17
3.4 Optical Interconnection using Dynamic Photorefractive Holograms .....	22
4.0 REFERENCES .....	25
APPENDIX 5.1: Optical Matrix-Vector Multiplication Through Four-Wave Mixing in Photorefractive Media .....	27
APPENDIX 5.2 Optical Matrix-Matrix Multiplication using Multi-Color Four-Wave Mixing .....	31



Accession For	
NTIS GRA&I	<input checked="checked" type="checkbox"/>
DTIC TAB	<input type="checkbox"/>
Unannounced	<input type="checkbox"/>
Justification	
By	
Distribution/	
Availability Codes	
Dist	Avail and/or Special
A-1	



## LIST OF FIGURES

	<u>Page</u>
Fig. 1	Matrix-matrix multiplication in four-wave mixing. .... 5
Fig. 2	Matrix-vector multiplication via four-wave mixing. .... 8
Fig. 3	Reconfigurable optical interconnection. .... 10
Fig. 4	Optical matrix-vector multiplication using photorefractive four-wave mixing .... 11
Fig. 5	Experimental results of optical matrix-vector multiplication using photorefractive four-wave mixing. .... 13
Fig. 6	Output of the detector monitoring the intensity of the optical beam representing the product vector. .... 14
Fig. 7	Decomposition of matrix-matrix multiplication into matrix-vector multiplication. .... 14
Fig. 8	Optical matrix-matrix multiplication via color multiplexing. .... 15
Fig. 9	The color encoding scheme used in our experimental demonstration of optical matrix-matrix multiplication for the case of $2 \times 2$ matrices. .... 16
Fig. 10	Experimental results for matrix-matrix multiplication using color-multiplexed four-wave mixing in a photorefractive crystal: (a) the spatial intensity pattern of the output prior to the scanning cylindrical optics; (b) the spatial pattern representing the final result. .... 16
Fig. 11	A schematic diagram illustrating the basic idea of four-wave mixing in a nonlinear medium located at the common Fourier plane of the input spatial pattern. .... 18
Fig. 12	A schematic illustration of convolution of two spatial patterns: (a) and (b) are the two input spatial patterns; (c) represents the resulting spatial convolution of the two inputs. .... 18
Fig. 13	A schematic diagram illustrating optical matrix-matrix multiplication by convolution for the case of $2 \times 2$ matrices: (a) matrix A and the mask $U_1$ to encode A; (b) matrix B and the mask $U_2$ to encode $B^T$ ; (c) the spatial pattern resulting from convolution of $U_1$ and $U_2$ . .... 19



## LIST OF FIGURES

	<u>Page</u>
Fig. 14    An illustration similar to Fig. 13 for the case when the dimensions of the matrices A, B and C are $2 \times 3$ , $3 \times 4$ and $2 \times 4$ , respectively. ....	20
Fig. 15    Experimental results for optical matrix-matrix multiplication by convolution via four-wave mixing in the spatial frequency domain. (a) and (b) are the matrix masks used for encoding the matrices. ....	21
Fig. 16    A schematic drawing of a $1 \times N$ optical interconnection using dynamic photorefractive holograms. $N = 4$ . ....	23
Fig. 17    A schematic drawing of a $N \times N$ optical interconnection using dynamic photorefractive holograms. $N = 4$ . ....	23



## 1.0 SUMMARY

### 1.1 Contract Description

This contract studies unique optical computing concepts which use nonlinear optical phenomena to perform matrix multiplication and to provide reconfigurable optical interconnection. The study focuses on the use of real-time holography in nonlinear media such as photorefractive crystals for optical computing.

### 1.2 Scientific Problem

By incorporating the parallel nature of optics in nonlinear media, it is possible to perform parallel matrix multiplication using four-wave mixing. In addition, the dynamic holography in nonlinear optical media provides a nature candidate for the reconfigurable interconnection. The general problem in this program is to generate and investigate new concepts which use these nonlinear optical phenomena for optical computing.

Specifically, this program investigates experimentally and theoretically the multiplication of matrices using optical four-wave mixing in nonlinear media, and the possibility of using such matrix multiplication for reconfigurable interconnection.

### 1.3 Progress

There are several areas of significant progress in the first year of this program that are directly related to the development of optical matrix multiplication and reconfigurable interconnection. These include:

1. First experimental demonstration of parallel matrix-vector multiplier using optical four-wave mixing in a barium titanate ( $\text{BaTiO}_3$ ) crystal.
2. First experimental demonstration of summation process inside the nonlinear media in matrix-vector multiplications.
3. Experimental demonstration of  $2 \times 2$  matrix-matrix multiplication using four-wave mixing in a  $\text{BaTiO}_3$  crystal.



SC5502.AR

4. Experimental demonstration of matrix-matrix multiplication using color multiplexing.
5. Experimental demonstration of matrix-matrix multiplication using convolution.
6. Development of a new scheme of reconfigurable optical interconnection which is energy-efficient.

#### 1.4 Publications and Presentations

"Optical Matrix-Vector Multiplication via Four-Wave Mixing in Photorefractive Media," Opt. Lett. 12, 138 (1987); Opt. Lett. 12, 373 (1987).

"Optical Matrix-Vector Multiplication Using Four-Wave Mixing," Paper MM5, OSA Annual Meeting (Oct. 1986, Seattle, WA), J. Opt. Soc. Am. A3 (13), 16 (1986).

"Optical Matrix-Matrix Multiplication Using Multicolor Four-Wave Mixing," Proc. SPIE, vol. 881, paper 38, to be presented at OE/LASE'88 (Jan. 10-17, 1988, Los Angeles, CA).

#### 1.5 Patent Disclosures

"Multicolor Matrix-Matrix Multiplier with  $N^3$  Parallelism," M. Khoshnevisan, A.E.T. Chiou and P. Yeh, Rockwell Patent Disclosure 87SC37.

"Matrix-Vector Multiplier using Photorefractive Phase Conjugators," P. Yeh, A.E.T. Chiou and M. Khoshnevisan, Rockwell Patent Disclosure 87SC46.

"Optical Matrix-Matrix Multiplier with  $N^3$  Parallelism by Spatial Convolution via Four-Wave Mixing," A.E.T. Chiou, Rockwell Patent Disclosure 87SC63.

"Reconfigurable Optical Interconnect using Dynamic Holograms," P. Yeh, Rockwell Patent Disclosure 87SC54.



## 2.0 TECHNICAL DISCUSSION

The technical problem addressed in this contract is the study of optical matrix multiplication and reconfigurable interconnection. By incorporating the parallel nature of optics in nonlinear media such as photorefractive crystals,<sup>1,2</sup> it is possible to perform parallel matrix multiplication using four-wave mixing. In addition, the dynamic holography in nonlinear optical media provides a nature candidate for the reconfigurable interconnection.<sup>3,4</sup>

Specifically, this program is aimed at the utilization of nonlinear optical phenomena such as phase conjugation and four-wave mixing in nonlinear media<sup>5-8</sup> to perform the matrix-vector and matrix-matrix multiplication. Photorefractive crystals such as BaTiO<sub>3</sub> and strontium barium niobate (SBN) were used as the nonlinear media.

Generally speaking, four-wave mixing is a nonlinear optical process in which three input waves mix to yield a fourth wave. In phase-matched four-wave mixing, the three input waves consist of two counterpropagating pump waves,  $E_1$  and  $E_2$ , and an arbitrary probe wave,  $E_3$ . All three couple through the third-order susceptibility,  $\chi^{(3)}$ , to yield a fourth wave,  $E_4$ , which is proportional to the product of  $E_1$ ,  $E_2$  and complex conjugate of  $E_3$ , and can be written as<sup>6</sup>

$$E_4 \propto \chi^{(3)} E_1 E_2 E_3^*$$

Such a four-wave mixing can be understood in terms of the recording and readout processes which occur in holography. In the nonlinear media, one of the pump waves and the probe wave form an interference pattern which, in turn, induces an index grating. The other pump wave is diffracted from this grating and generates the fourth wave. The formation and readout processes take place at the same time. Thus, four-wave mixing is sometimes referred to as a real-time holography.

By using four-wave mixing in nonlinear media, multiplication of signals can take place in a subpicosecond time scale. In addition, if we use the parallel nature of optical waves, each wave can carry spatial information for the purpose of image processing using the two transverse dimensions. Such an application of four-wave mixing to real-time image processing was recently reported using BSO crystals.<sup>9</sup> In what follows,





SC5502.AR

we will describe some unique concepts which use the two transverse dimensions to carry the matrix information for the purpose of matrix multiplication and reconfigurable interconnection.

## 2.1 Matrix-Matrix Multiplication

The matrix multiplication<sup>10-12</sup> between two  $N \times N$  matrices can be stated as follows:

$$C = AB \quad (1)$$

where

$$C_{ij} = \sum_k A_{ik} B_{kj} \quad (2)$$

Note that a matrix multiplication consists of two main operations, a parallel multiplication and an addition.

Referring to Fig. 1a, let us consider a four-wave mixing configuration which is suitable for matrix multiplication. Beam 1 and Beam 2 contain the information about the two matrices  $A(x,z)$  and  $B(z,y)$ , respectively. Beam 1 is propagating along the  $y$ -axis, and Beam 2 is propagating along the  $x$ -axis. These directions are chosen for the sake of clarity in introducing the concept. They are not the only directions for matrix multiplication. Also, these matrices can be either continuous or discrete. In the discrete case, each beam consists of a matrix of beamlets, as shown in Fig. 1b.

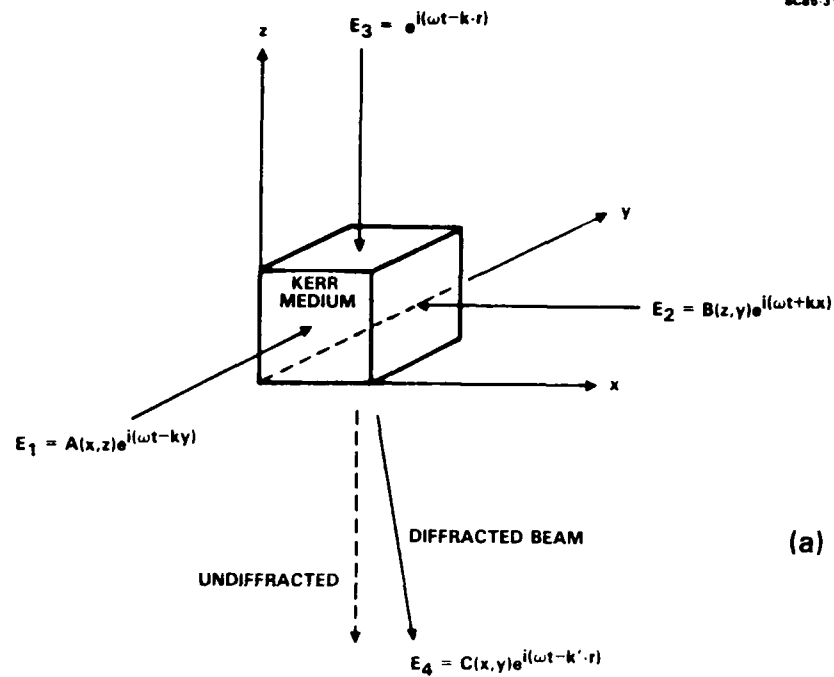
In the nonlinear medium, these two matrix-carrying beams form an interference pattern. As a result of the nonlinear response of the medium, a volume grating is formed. This grating contains information about the product of the matrix elements of these two matrices, and can be written as:

$$\Delta n = n_2 A(x,z) B^*(z,y) e^{i(\mathbf{K} \cdot \mathbf{r})} + \text{c.c.} \quad , \quad (3)$$



SC5502.AR

SC85-31538



(a)

$$C(x,y) = \int A(x,z)B^*(z,y)dz$$

SC85-31540

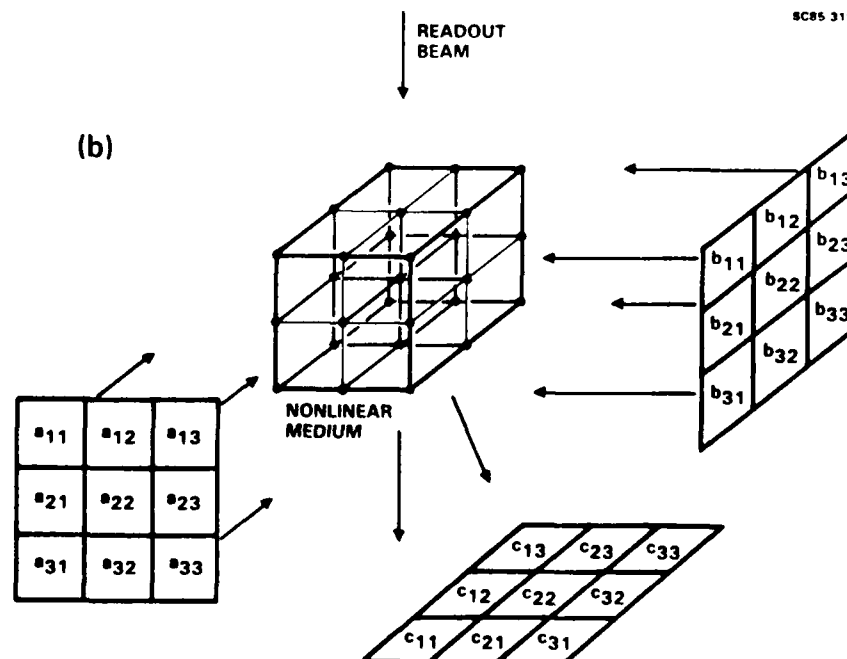


Fig. 1 Matrix-matrix multiplication in four-wave mixing.



SC5502.AR

where  $\mathbf{K}$  is the difference of the wavevector of the matrix-carrying beams and  $cc$  represents complex conjugation. The parameter  $n_2$  is the Kerr coefficient and is proportional to the third-order susceptibility  $\chi^{(3)}$  of the medium. Note that the nonlinear response of the medium serves the purpose of parallel multiplication.

The volume grating is then read out by a third beam which can simply be a plane wave. The diffracted beam consists of the integrated contribution from each part of the grating along the beam path, and thus can be written

$$C(x,y) = \int A(x,z)B^*(z,y)dz \quad (4)$$

where the integration is carried out along the beam path. Note that the integration completes the operation of matrix multiplication. The information about the product of these two matrices is now impressed on the transverse spatial distribution of the diffracted beam.

Due to the phase matching requirement, the readout beam must be incident along the directions which satisfy the Bragg diffraction condition to achieve high efficiency. In anisotropic nonlinear media, the polarization states, as well as the direction of propagation, can be chosen such that the largest of the nonlinear susceptibilities is fully utilized.

The four-wave mixing can be either degenerate or nondegenerate. In the degenerate case, all the beams have the same frequency. In the nondegenerate case, the frequencies of the beams can be slightly different. This may be useful for the purpose of separating the diffracted beam from the undiffracted portion.

To illustrate the information capacity of such a nonlinear optical matrix multiplication, let us consider a four-wave mixing process using an Ar ion laser at 4880 Å in a medium of a 1 cm cube. The grating space is of the order of 0.5  $\mu\text{m}$ . Thus, 10  $\mu\text{m}$  x 10  $\mu\text{m}$  is enough for each pixel of information. In other words, a 1 cm cube is capable of handling 1000 x 1000 matrices. With a material response time of 1 ns, such a matrix multiplication has a potential data throughput rate of quadrillion bits per second ( $10^{15}$  bits/s)!



## 2.2 Matrix-Vector Multiplication

Another scheme as shown in Fig. 2 is suitable for matrix-vector multiplication.<sup>10-12</sup> Here, as an example, let us consider a discrete case in which we need to carry out the multiplication of an N-element vector and an N x N matrix. The vector is fanned out into N-rows of identical vectors. These N x N small beams are directed to a non-linear medium. The matrix which also contains N x N small beams is also directed to the medium in such a way that each beam of the matrix is counterpropagating in a direction relative to the corresponding beam of the vector. Thus, in the medium, there are N x N spatially separated regions which are pumped each by a pair of counterpropagating beams. Now, N x N probing beams are directed into the medium in such a way that each probe beam will propagate through an intersection region. The probe beams will be "plane wave" beamlets propagating in parallel. As a result of the four-wave mixing, each probe beam will generate a phase-conjugated beam which, within a proportional factor, can be written  $M(i,j)a(j)$ . By using a cylindrical lens, a summation over j can be obtained. Thus, we have

$$b(i) = \sum_j M(i,j)a(j) \quad (5)$$

where  $a(j)$  is the j-th element of the vector  $\vec{a}$  and  $M(i,j)$  is the matrix element. Such a scheme for matrix-vector multiplication can also be used for matrix-matrix multiplication by decomposing a matrix into column vectors and then multiplying the matrix with each of the column vectors.

## 2.3 Reconfigurable Optical Interconnection

Optical interconnection will play a key role in both the optical computing and VLSI systems.<sup>3,4,13</sup> There are many advantages of optical interconnect. Optical systems can have high space-bandwidth and time-bandwidth products; hence, many independent channels that could be exploited for demanding computations. Optical processors are inherently two-dimensional and parallel. Optical signals can propagate through each other in separate channels with essentially no interaction. Optical signals can also propagate in parallel channels without any interference and crosstalk. In the VLSI systems, optical interconnect can be used to solve the problem of communication, as well as the clock distribution.



SC5502.AR

SC85-31541

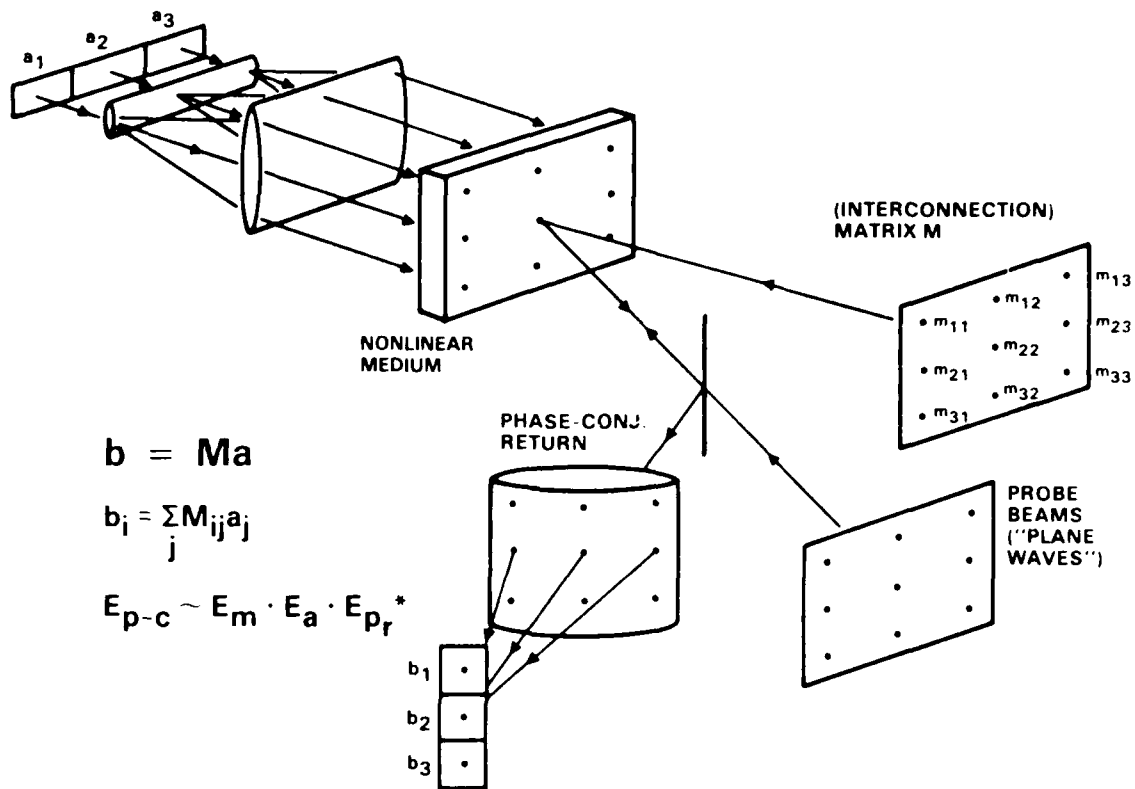


Fig. 2 Matrix-vector multiplication via four-wave mixing.

Computer-generated holograms (CGH) can be used for fixed optical interconnect. The most general CGH consists of a two-dimensional array of subholograms. Each subhologram is capable of diffracting a gate output to any gate or combination of gate inputs. Such a fixed interconnect pattern is adequate for many applications, including the point operation, matrix operation, the clock distribution and a globally synchronous systolic processor. However, there are many situations in which a dynamic optical interconnect is required.

In Fourier transform and sorting, every element of an output array is affected by all the elements of the input array, and conversely, each element of the input array affects all elements of the output array. In addition, the interconnections change at different stages of the computation. Thus, these operations require global and dynamic interconnection between different elements of the input array.



SC5502.AR

In image restoration and pattern recognition, the interconnect patterns could be data-dependent, making it impossible to foresee the interconnect requirements at different stages of processing without having foreknowledge of the input. The computational throughput of parallel processor implementing these types of operation will be critically affected by the availability of a dynamic and global interconnect network.

In Fourier transform and sorting, the requirement for dynamic interconnect can be avoided by resorting to a fixed but global interconnect pattern known as the "perfect shuffle". In the area of image restoration and pattern recognition, there is a minimum amount of regularity and structure. In addition, there is a possible data and time dependency in the interconnect requirements. A global and reconfigurable interconnect network will be vital to achieving high throughput and high efficiency with parallel processors implementing these operations.

The most general interconnect system is one in which any gate output can be connected to the input of any gate or combination of gates (see Fig. 3). The effect of such an interconnect can be represented by the matrix equation

$$O = M I \quad (6)$$

where  $I$  is a vector representing the two-dimensional input array,  $M$  is the matrix representing the interconnect, and  $O$  is a vector representing the output array. In digital optical computing,<sup>14,15</sup> the input array is actually the gate output array. Each matrix element  $(i,j)$  is nonzero if, and only if, there is a connection between pixel  $j$  of the input array and pixel  $i$  of the output array. The matrix-vector multiplication technique described in Section 2.2 can be used as an optical interconnect, which provides both local and global communication between the gate input and gate output. In the VLSI systems, the vectors  $I$  may consist of  $N$  laser beams, each containing a stream of data from a processor, and the vector  $O$  represents the output laser beams, each feeding into a processor. The main advantage of using such nonlinear matrix-vector multiplication for interconnection is that the matrix  $M$  can be easily changed for the purpose of reconfiguring the interconnect.



SC5502.AR

SC85-31594

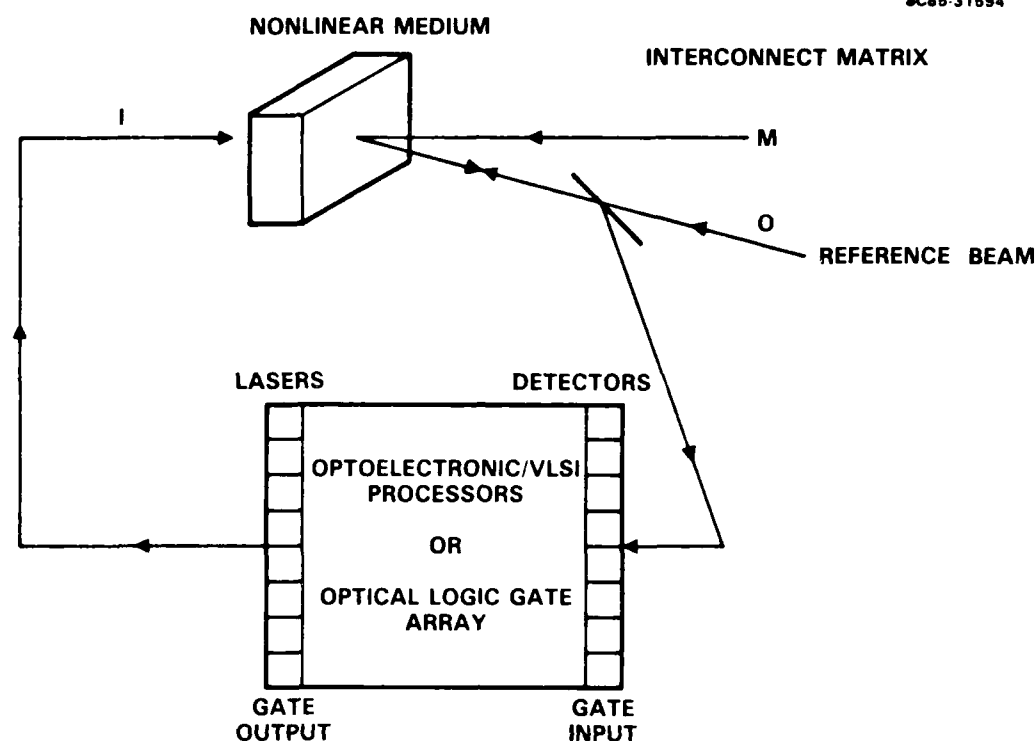


Fig. 3 Reconfigurable optical interconnection.

Equation (6) can be generalized such that both the input array  $I$  and the output array  $O$  are two-dimensional matrices. In that case, the most general interconnect matrix  $M$  must be four-dimensional (i.e., tensor of rank four). Each matrix element  $(ijkl)$  represents the connection between pixel  $(ij)$  of the output array and pixel  $(kl)$  of the input array. Because of the two-dimensional nature of optical waves, it is desirable to represent the matrix  $M$  by a two-dimensional array of two-dimensional submatrices. Thus, the matrix-matrix multiplication described in Section 2.1 can be used for reconfigurable optical interconnect which provides the most general interconnection pattern. While this interconnection scheme allows complete generality, a price is paid in terms of the space-bandwidth product requirements on the nonlinear media.



### 3.0 PROGRESS

#### 3.1 Matrix-Vector Multiplication

In our earlier demonstration of optical matrix-vector multiplication (see Appendix 5.1), we have used optical phase conjugation via nonlinear four-wave mixing in a photorefractive  $\text{BaTiO}_3$  crystal to perform pixel-by-pixel multiplication. The summation required to obtain matrix-vector products is performed subsequently by a cylindrical lens external to the nonlinear medium. With a slight modification of the experimental geometry, we have successfully demonstrated that both the pixel-by-pixel product and the summation can be done inside the nonlinear medium to achieve the desired matrix-vector product without an external cylindrical lens.

The top view of the new experimental geometry is illustrated schematically in Fig. 4. The readout vector in this case consists of a vertical column of beamlets with equal intensity and enter the crystal at an oblique angle such that each beamlet traverses, inside the crystal, all the counterpropagating pumping beamlets at the same

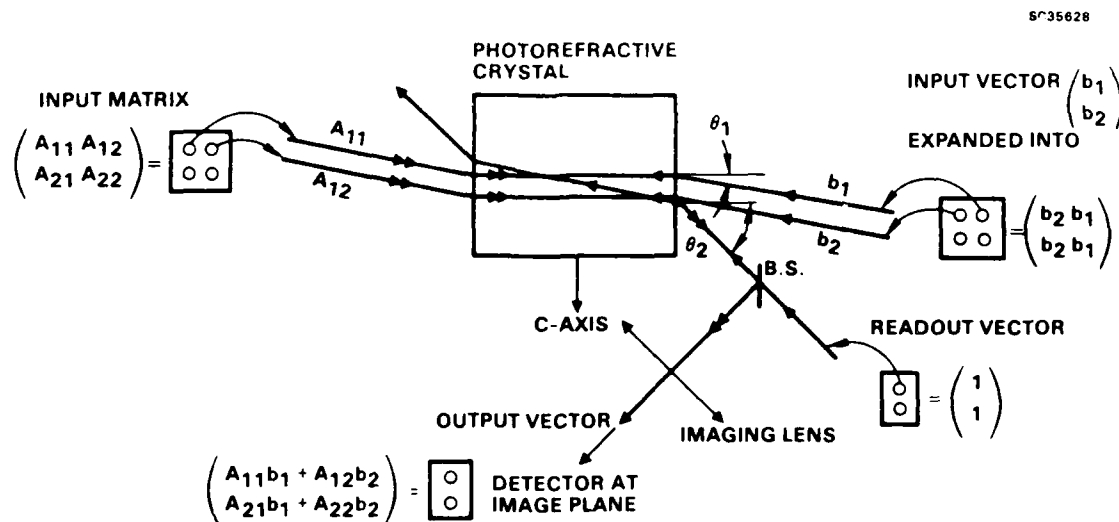


Fig. 4 Optical matrix-vector multiplication using photorefractive four-wave mixing.





SC5502.AR

horizontal plane. As the proper elements of the matrix and the vector are encoded in the two counterpropagating beams via the appropriate masks, the phase-conjugate output of each beamlet consists of the sum of the product resulting from each individual encounter. From a pure geometrical point of view, the probe beam (i.e., the readout vector) can conveniently be injected (from c-face of the crystal) perpendicular to the counter-propagating pumping beams. The tensor nature of the photorefractive grating,<sup>5</sup> however, does not allow coupling in such a geometry, except for cubic crystals such as GaAs.

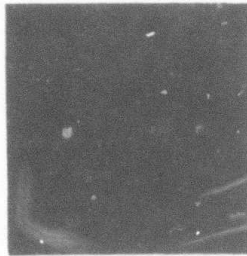
The experimental result for the multiplication of a  $4 \times 4$  binary matrix and a  $4 \times 1$  binary vector is shown in Fig. 5. The magnified images of the masks used to encode the matrix, the vector and the probe are shown in Figs. 5a, b and c, respectively. The experimental results representing the final matrix-vector product is shown in Fig. 5d. The relative intensity of each output spot representing the element of the product vector is shown in Fig. 6. Due to the slow response time (or the order of second for optical intensity of the order of a few tens of milliwatt/cm<sup>2</sup>) and the consequential sensitivity to environmental changes of the photorefractive process, the output intensity fluctuates significantly. The  $\pm 25\%$  noise level is likely to limit its application to binary operation only.

### 3.2 Matrix-Matrix Multiplication via Color Multiplexing

We have also extended our experimental demonstration on matrix-vector multiplication to matrix-matrix multiplication by color multiplexing (see Appendix 5.2). The basic idea is to decompose the problem into matrix-vector multiplications, as shown in Fig. 7, and carry out all the matrix-vector multiplications simultaneously in parallel by using color multiplexing. Note that each of the matrix-matrix operations shown on the right-hand side of the equation in Fig. 7 is in fact a matrix-vector multiplication. The basic principle of color multiplexing used to encode the component vectors with different colors is illustrated in Fig. 8 for the case of  $4 \times 4$  matrices. Each row vector of the matrix  $M_1$  is illuminated by one color, and all the color components are then combined by the prism (angular multiplexing) into a single row prior to further expansion by anamorphic optics (not shown in the figure) to match the mask representing the second matrix. After proper element-by-element multiplications and summation (summing optics omitted) into the column, the resulting multicolor output is demultiplexed into different color components that together represent the final product.

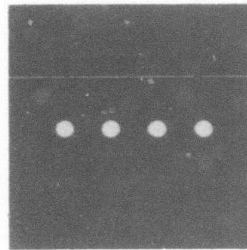


SC37356



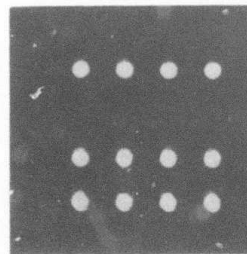
(d)  
OUTPUT  
VECTOR

$$\begin{bmatrix} 3 \\ 0 \\ 1 \\ 2 \end{bmatrix}$$



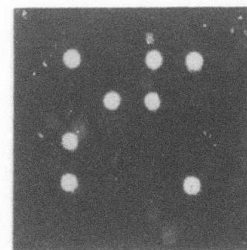
(c)  
READ OUT  
(PROBE)  
VECTOR

=



(b)  
INPUT VECTOR  
(EXPANDED INTO  
MATRIX FORM)

$$\begin{bmatrix} 1 & 1 & 0 & 1 \\ 1 & 1 & 0 & 1 \end{bmatrix}$$



(a)  
INPUT MATRIX

$$\begin{bmatrix} 1 & 1 & 0 & 1 \\ 0 & 0 & 1 & 0 \\ 0 & 0 & 1 & 1 \\ 1 & 0 & 0 & 1 \end{bmatrix}$$

Fig. 5 Experimental results of optical matrix-vector multiplication using photorefractive four-wave mixing.



SC5502.AR

BC37366

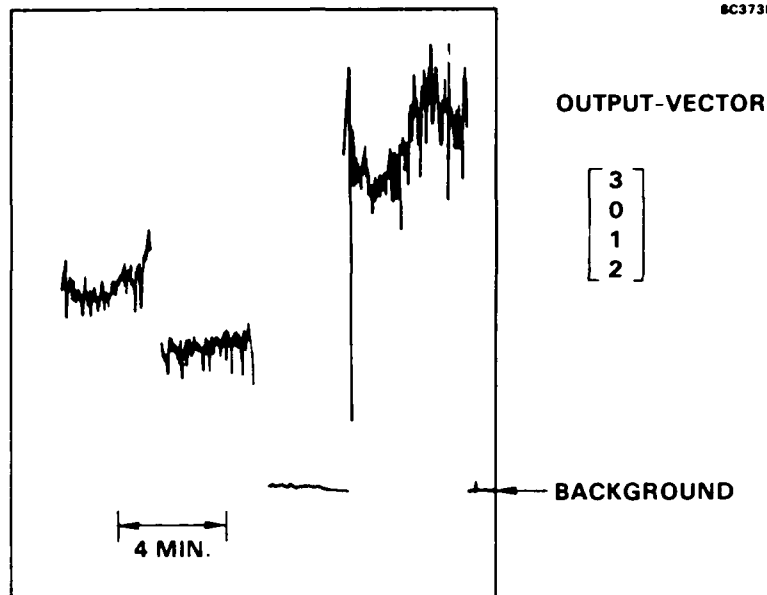


Fig. 6 Output of the detector monitoring the intensity of the optical beam representing the product vector.

$$\begin{bmatrix} m_{11} & m_{12} & m_{13} \\ m_{21} & m_{22} & m_{23} \\ m_{31} & m_{32} & m_{33} \end{bmatrix} \begin{bmatrix} a_{11} & a_{12} & a_{13} \\ a_{21} & a_{22} & a_{23} \\ a_{31} & a_{32} & a_{33} \end{bmatrix} = \begin{bmatrix} m_{11} & m_{12} & m_{13} \\ m_{21} & m_{22} & m_{23} \\ m_{31} & m_{32} & m_{33} \end{bmatrix} \begin{bmatrix} a_{11} & 0 & 0 \\ a_{21} & 0 & 0 \\ a_{31} & 0 & 0 \end{bmatrix} \\
 + \begin{bmatrix} m_{11} & m_{12} & m_{13} \\ m_{21} & m_{22} & m_{23} \\ m_{31} & m_{32} & m_{33} \end{bmatrix} \begin{bmatrix} 0 & a_{12} & 0 \\ 0 & a_{22} & 0 \\ 0 & a_{32} & 0 \end{bmatrix} \\
 + \begin{bmatrix} m_{11} & m_{12} & m_{13} \\ m_{21} & m_{22} & m_{23} \\ m_{31} & m_{32} & m_{33} \end{bmatrix} \begin{bmatrix} 0 & 0 & a_{13} \\ 0 & 0 & a_{23} \\ 0 & 0 & a_{33} \end{bmatrix}$$

Fig. 7 Decomposition of matrix-matrix multiplication into matrix-vector multiplication.



SC5502.AR

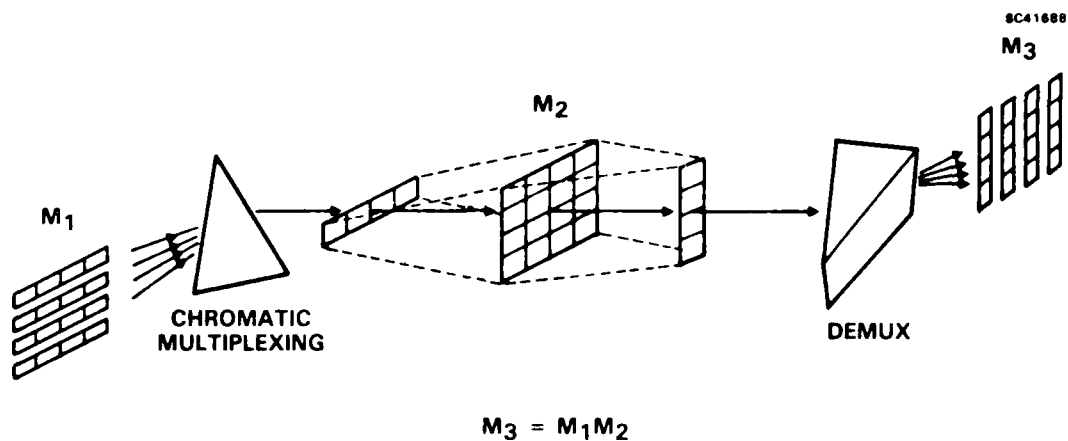


Fig. 8 Optical matrix-matrix multiplication via color multiplexing.

Using an argon ion laser that oscillates simultaneously at five colors in the blue-green and a  $\text{BaTiO}_3$  crystal, we have demonstrated the principle described above for the case of  $2 \times 2$  matrices. The two matrices  $M$  and  $A$  and the corresponding color encoding schemes are shown in Fig. 9, and the experimental results are given in Fig. 10. The spatial pattern in Fig. 10a is the output prior to the summing cylindrical optics; the pattern in Fig. 10b is the final result. The relative intensity of each spot is also shown in the figure.

An important practical issue is the maximum dimension ( $N$ ) of the matrices allowed for this approach. For  $N \leq 5$ , photorefractive materials such as  $\text{BaTiO}_3$  or SBN can be used. For larger  $N$ , however, it is expected that the diffraction efficiency of the hologram for any given color will be adversely affected by the erasure effects of the other  $N-1$  beams and by the superposition of the other  $N-1$  holograms. For larger values of  $N$ , modification such as the use of near-resonance multilayer nonlinear medium (multiple quantum well, for instance) may be helpful.



SC5502.AR

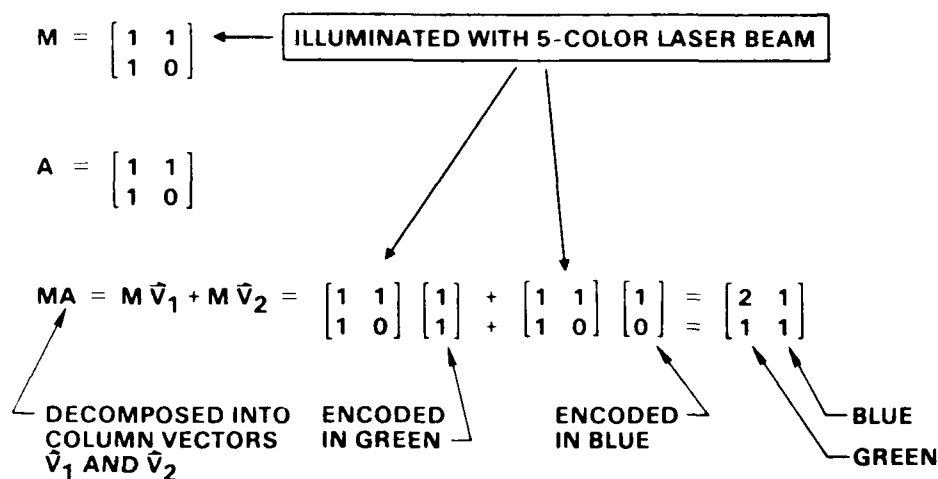


Fig. 9 The color encoding scheme used in our experimental demonstration of optical matrix-matrix multiplication for the case of  $2 \times 2$  matrices.

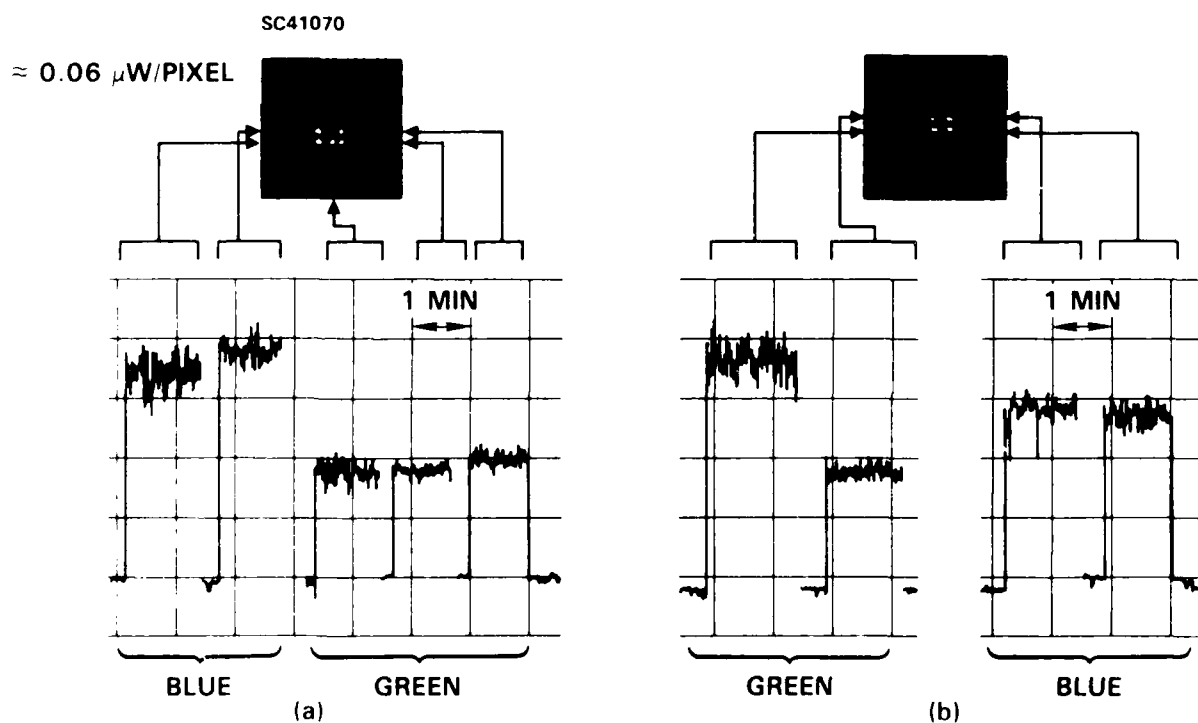


Fig. 10 Experimental results for matrix-matrix multiplication using color-multiplexed four-wave mixing in a photorefractive crystal: (a) the spatial intensity pattern of the output prior to the scanning cylindrical optics; (b) the spatial pattern representing the final result.



### 3.3 Matrix-Matrix Multiplication using Spatial Convolution

In addition to the matrix-matrix multiplication using color-multiplexed four-wave mixing described in the previous section, we have also successfully demonstrated another scheme for matrix-matrix multiplication using spatial convolution via four-wave mixing. From the experimental point of view, the key difference between this approach and the others described above is that the nonlinear crystal is now located at the common Fourier plane, rather than the common image plane, of the input matrix masks. The encoding scheme, as explained in the following paragraphs, is also different from those used in the earlier approaches. From the conceptual point of view, matrix-matrix multiplication in full parallelism is achieved by space-multiplexing via spatial convolution using degenerate four-wave mixing.

White and Yariv<sup>16</sup> have demonstrated that (spatial) convolution and correlation of two (two-dimensional) patterns can be achieved in real time by four-wave mixing in the common Fourier plane of the input patterns and recording the phase-conjugated output at the corresponding object plane. A typical experimental configuration is shown schematically in Fig. 11. Specifically, if U3 is a small aperture simulating a point source (or a delta function), a pattern representing the convolution of U1 and U2 ( $U1 * U2$ ) is observed in the output plane. An illustrative example is given in Fig. 12. The design of U1 and U2 to represent two matrices so that their product is represented by  $U1 * U2$  is explained in the following paragraphs.

For simplicity and clarity, let us consider the simplest cases of two matrices A and B, both of dimension 2 x 2, and their product  $C = AB$  given below.

$$A = \begin{pmatrix} a_{11} & a_{12} \\ a_{21} & a_{22} \end{pmatrix}$$

$$B = \begin{pmatrix} b_{11} & b_{12} \\ b_{21} & b_{22} \end{pmatrix}$$

(7)

$$C = AB = \begin{pmatrix} c_{11} & c_{12} \\ c_{21} & c_{22} \end{pmatrix} = \begin{pmatrix} a_{11}b_{11} + a_{12}b_{21} & a_{11}b_{12} + a_{12}b_{22} \\ a_{21}b_{11} + a_{22}b_{21} & a_{21}b_{12} + a_{22}b_{22} \end{pmatrix}$$



SC5502.AR

SC41299

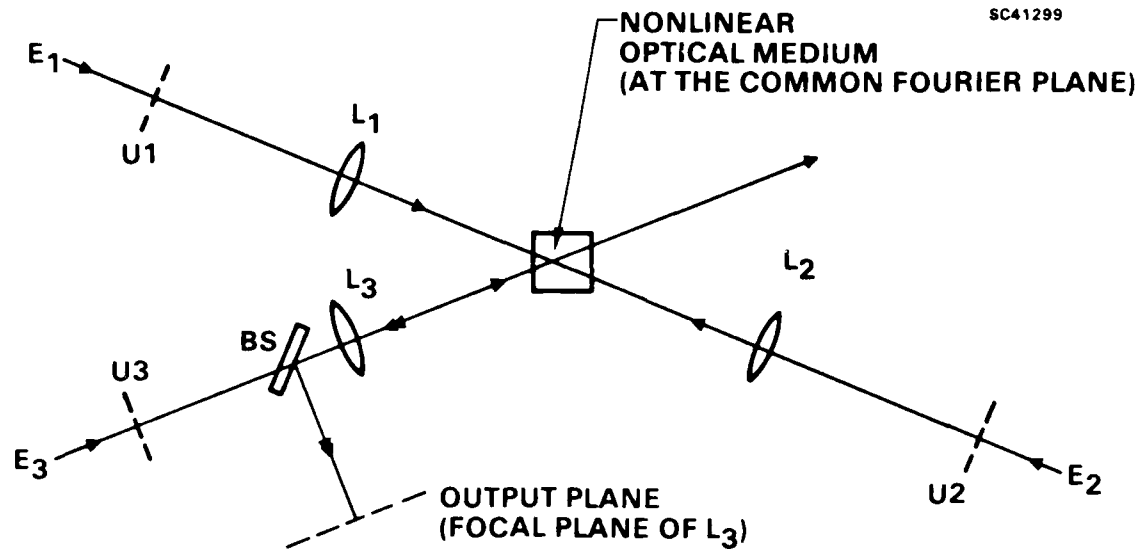


Fig. 11 A schematic diagram illustrating the basic idea of four-wave mixing in a non-linear medium located at the common Fourier plane of the input spatial pattern.

SC4129F

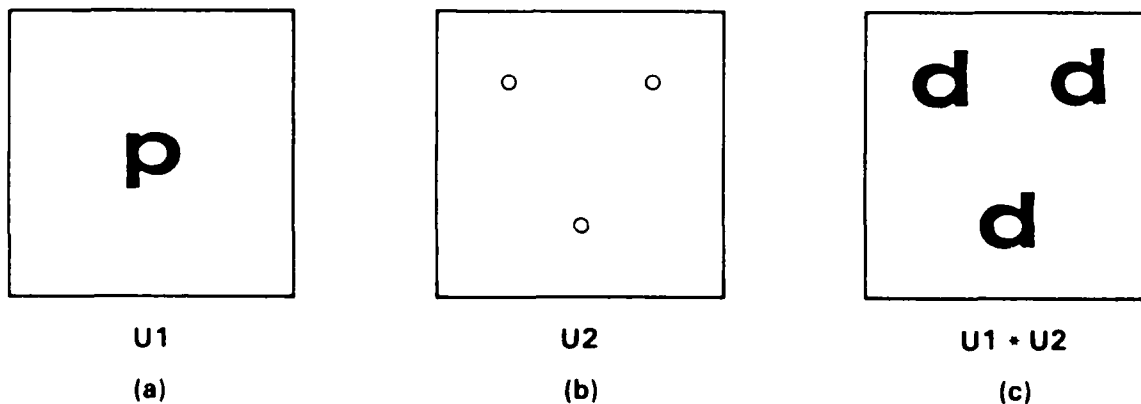


Fig. 12 A schematic illustration of convolution of two spatial patterns: (a) and (b) are the two input spatial patterns; (c) represents the resulting spatial convolution of the two inputs.



SC5502.AR

A transparency  $U_1$  consists of four small apertures, each with its intensity transmittance proportional to each of the matrix element  $a_{ij}$  is shown in Fig. 13a. A similar transparency  $U_2$  corresponding to the transpose of B (i.e., rows and columns interchanged) is shown in Fig. 13b. Note that the vertical distance between the elements in  $U_1$  is designed so that it is considerably larger than that in  $U_2$ , while the horizontal distances between the elements are identical in  $U_1$  and  $U_2$ . Note also that the dashed rectangular box connecting the four elements in  $U_2$  is an artifact to facilitate the following explanation and should be ignored in the actual design. By comparing Figs. 12 and 13, it is straightforward to see how the quadruplet of the dashed rectangular box is formed at the corresponding position in Fig. 13c as a result of the two-dimensional spatial convolution. As noted before, all the dashed lines in Fig. 13c are artifacts and the actual result should show only the corners of each box, i.e., a total of 16 spots with the intensity of each proportional to the cross product of all the elements in A and those in B. The four doublets lying along the Y-axis in Fig. 13c are drawn slightly offset from the axis to

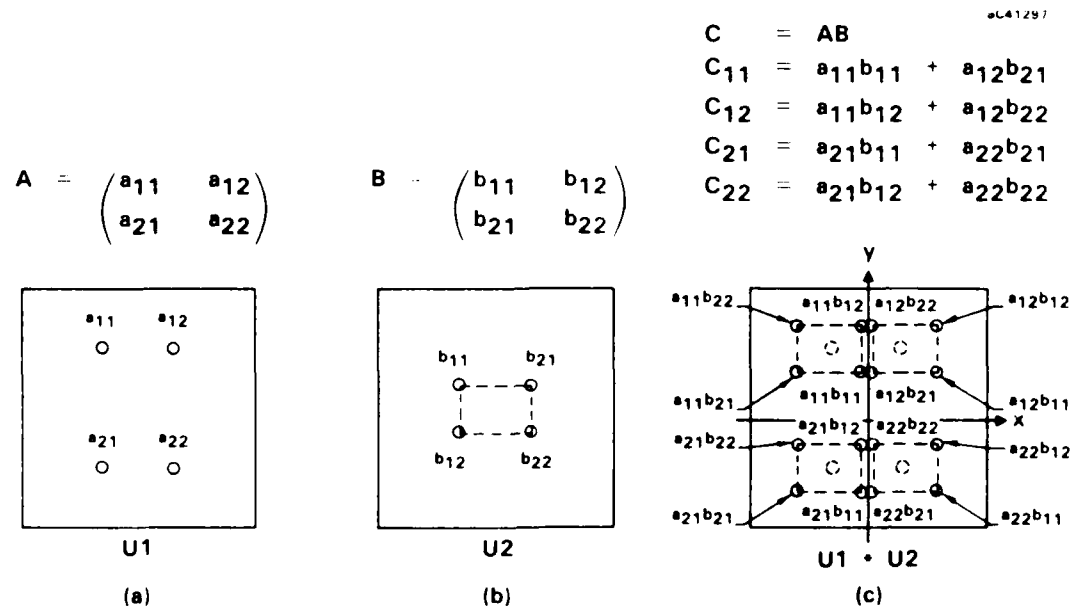


Fig. 13 A schematic diagram illustrating optical matrix-matrix multiplication by convolution for the case of  $2 \times 2$  matrices: (a) matrix A and the mask  $U_1$  to encode A; (b) matrix B and the mask  $U_2$  to encode  $B^T$ ; (c) the spatial pattern resulting from convolution of  $U_1$  and  $U_2$ .





SC5502.AR

expose the individual component. In practice, the two components of each doublet are spatially overlapping on the Y-axis. The intensity of the four doublets, from top to bottom, on the Y-axis are proportional to  $c_{12}$ ,  $c_{11}$ ,  $c_{22}$  and  $c_{21}$ , respectively. The eight cross terms that do not contribute to the matrix-matrix multiplication can be filtered out easily as they are physically separated from the Y-axis.

Another example illustrating the case of multiplying a  $2 \times 3$  matrix with a  $3 \times 4$  matrix is shown in Fig. 14. Note that all the cross terms that do not contribute to the matrix-matrix product are omitted in Fig. 14c for the sake of clarity.

Using an argon ion laser ( $5145\text{\AA}$ ) and a  $\text{BaTiO}_3$  crystal, we have experimentally demonstrated the concept described above for the case of  $2 \times 2$  matrices. The images of the masks used to encode the two matrices A and B are shown in Figs. 15a and 15b, respectively. The experimental result representing the product is shown in Fig. 15c. An

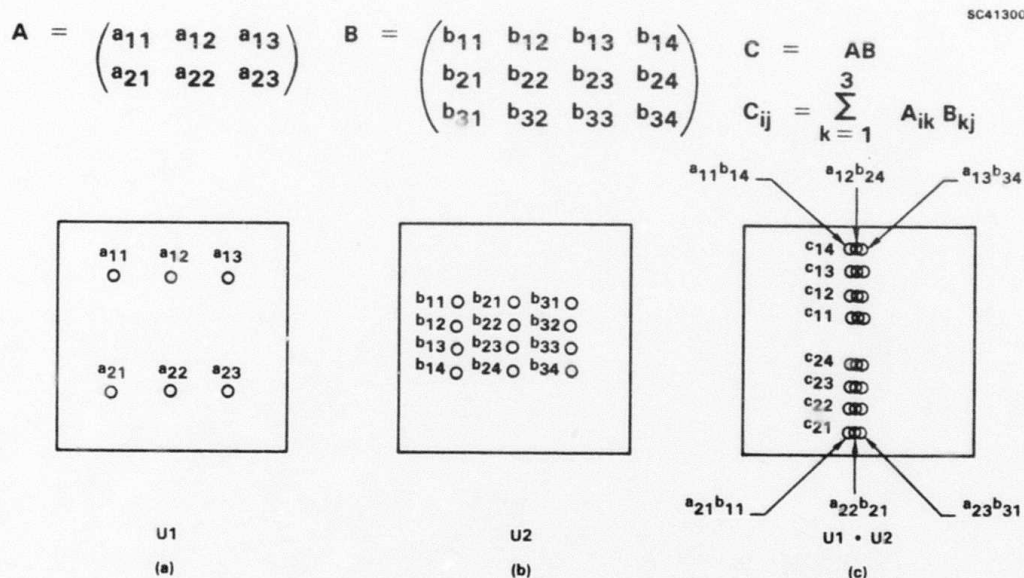


Fig. 14 An illustration similar to Fig. 13 for the case when the dimensions of the matrices A, B and C are  $2 \times 3$ ,  $3 \times 4$  and  $2 \times 4$ , respectively.

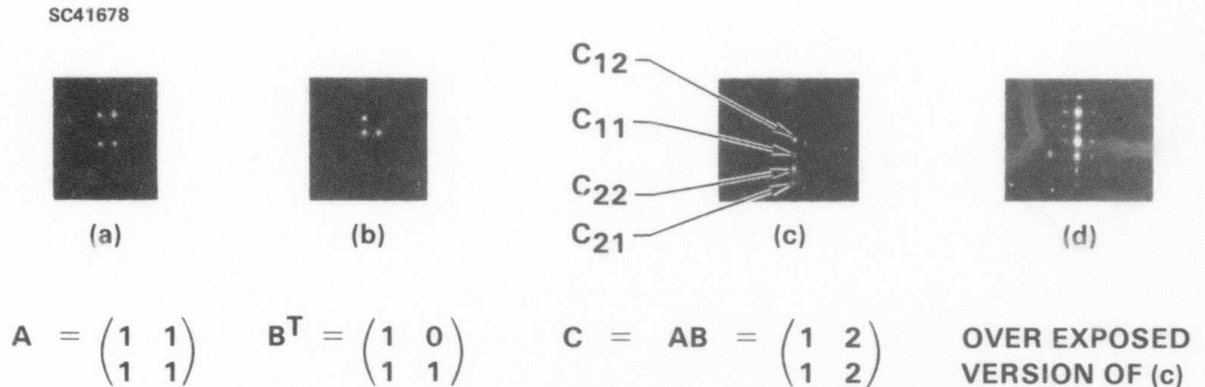


Fig. 15 Experimental results for optical matrix-matrix multiplication by convolution via four-wave mixing in the spatial frequency domain. (a) and (b) are the matrix masks used for encoding the matrices  $A$  and  $B^T$ ; (c) shows the result of their spatial convolution; (d) is an overexposed version of (c) to reveal the cross terms that do not contribute to the matrix product.

overexposed version of Fig. 15c is shown in Fig. 15d to reveal the noise resulting from the other cross terms that do not contribute to the matrix product.

In principle, the basic concept described above can be applied to the multiplication of a matrix (of any dimension  $m \times n$ ) and a compatible matrix  $B$  (of dimension  $n \times p$ ). In practice, the signal-to-noise (S/N) ratio is expected to degrade as the dimension of the matrix increases. The problem of S/N is less serious in the mixed binary mode. The major advantage of this scheme is the full parallelism achieved with relatively simple optical arrangements. From the technological point of view, the fact that all the output elements lie on a straight line can be significant, since this allows one to use a linear detector array instead of a 2-D array for output detection.



SC5502.AR

### 3.4 Optical Interconnection using Dynamic Photorefractive Holograms

During the first year of the program, we have also developed a new concept of reconfigurable optical interconnection using photorefractive holograms. This new scheme provides an optical interconnection between an array of laser sources and an array of detectors with a very high energy efficiency.

Reconfigurable interconnection linking laser arrays and detector arrays plays a key role in optical computing. Conceptually, such interconnection can be achieved by using an optical matrix-vector multiplication.

$$v' = M v \quad (8)$$

where  $v$  is the input vector representing the signals carried by the array of lasers, and  $v'$  is the output vector representing the signals carried by the array of detectors. The matrix  $M$  represents the interconnection pattern. When a transparency or spatial light modulator (SLM) is used as the interconnection pattern, a large fraction of energy is absorbed by the transparency or SLM. This energy loss increases as the dimension of the array increases. Often, the fractional energy loss can be as large as  $(N-1)/N$ , where  $N$  is the dimension of the array. For a  $1000 \times 1000$  crossbar switch, the loss due to fanout can be as big as 99.9%. This is not acceptable in high-speed computing because signals are passing through the SLM billion times per second and the energy loss can be enormous.

Referring to Figs. 16 and 17, we describe a new method of reconfigurable optical interconnection which uses the nonreciprocal energy transfer in photorefractive two-wave mixing to improve the energy efficiency. Figure 16 describes a one-dimensional case for the sake of clarity in explaining the concept. A small fraction of a laser beam is coupled out of the beam by using a beam splitter. This small fraction (called probe beam) is then expanded by using a cylindrical lens and passes through the spatial SLM. In the example shown, the laser beam is to connect to Detectors  $b$  and  $d$  as prescribed by the SLM. The transmitted beam is then recombined with the main beam inside a photorefractive crystal. As a result of nonreciprocal energy coupling, almost all the energy in the main beam is transferred to the probe beam which carries the interconnection pattern. The results is an optical interconnection with high energy efficiency. Figure 17 describes the reconfigurable interconnection for laser arrays and detector arrays. In the



SC5502.AR

SC41697

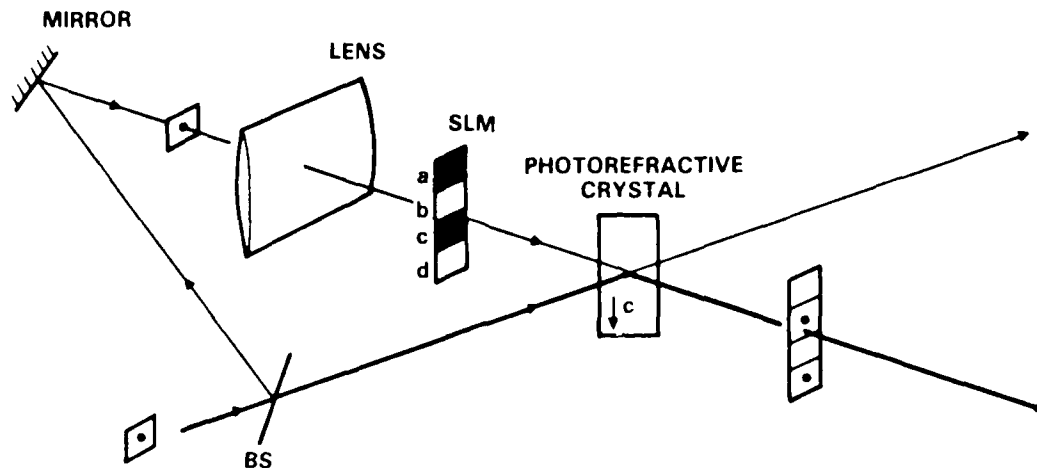


Fig. 16 A schematic drawing of a 1 x N optical interconnection using dynamic photorefractive holograms. N = 4.

SC41698

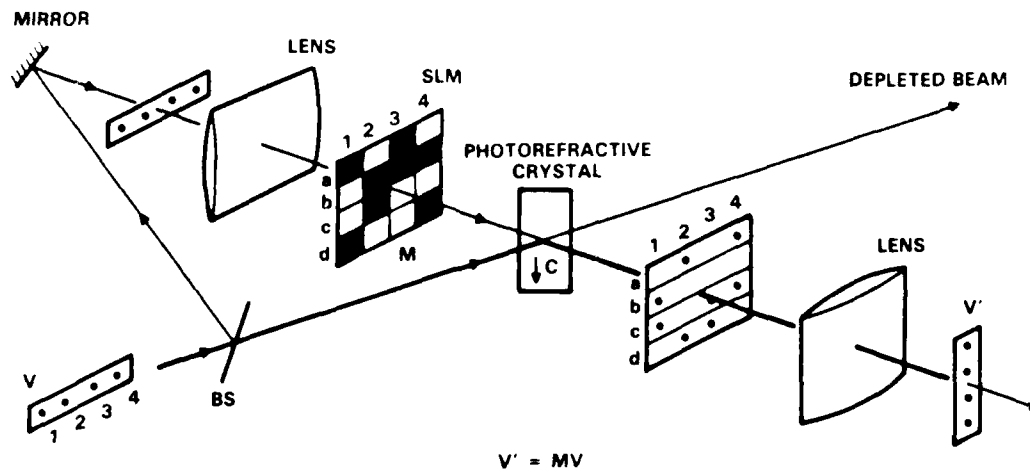


Fig. 17 A schematic drawing of a N x N optical interconnection using dynamic photorefractive holograms. N = 4.



SC5502.AR

example (a  $4 \times 4$  interconnection) shown, Laser 1 is to connect to Detectors b and c, Laser 2 is to connect to Detectors a and d, Laser 3 is to connect to Detectors c and d, Laser 4 is to connect to Detector a and c. A cylindrical lens is used to focus the two-dimensional array of beams into a vector (one-dimensional array). As a result, Detector a receives signals from Lasers 2 and 4, Detector b receives signals from Laser 1, Detector c receives signals from Lasers 1, 3 and 4, and Detector d receives signals from Lasers 2 and 3. Such a concept can be extended to interconnect NL lasers with ND detectors where NL and ND are two large numbers.

The interconnection can be reconfigured by using a different SLM pattern. The energy loss due to SLM is no more than the reflectivity of the beam splitter plus the material bulk absorption due to the photorefractive crystals. The beam splitter can be chosen such that the reflectivity is small (e.g., 5% or less) so that such energy loss is minimized. The hologram formation time will limit the reconfiguration time. Once the interconnection pattern is formed inside the photorefractive crystal as a hologram, such a scheme is capable of providing the interconnection for high data rate transmission. In such an interconnection, the output of each laser can be input to any one or all of the detectors.

Optical phase conjugation can also be used in conjunction with the two-wave mixing to correct for any phase aberration that may be caused by the crystal imperfection.<sup>17</sup>



#### 4.0 REFERENCES

1. V.L. Vinetskii, N.V. Kukhtarev, S.G. Odulov and M.S. Soskin, "Dynamic Self-Diffraction of Coherent Light Beams," *Sov. Phys. Usp.* 22, 742 (1979).
2. N.V. Kukhtarev, V.B. Markov, S.G. Odulov, M.S. Soskin and V.L. Vinetskii, "Holographic Storage in Electro-Optic Crystals. Beam Coupling and Light Amplification," *Ferroelectrics* 22, 949 (1979).
3. J.A. Neff, "The Role of Optics in Future Computational Systems," Topical Meeting on Optical Computing, March 18-10, Incline Village, NV, 1985.
4. J.W. Goodman, F.J. Leonberger, S-Y. Kung and R.A. Athale, "Optical Interconnections for VLSI Systems," *Proc. IEEE* 72, 850-866 (1984).
5. See, for example, A. Yariv and P. Yeh, "Optical Waves in Crystals" (Wiley, 1984), Chapters 12 and 13.
6. Y.R. Shen, "Principles of Nonlinear Optics (Wiley, 1984).
7. A. Yariv, "IEEE J. Quantum Elect. QE14, 650 (1978).
- 8.. C.R. Giuliano, *Physics Today* 27 (April, 1981).
9. J.O. White and A. Yariv, *Appl. Phys. Lett.* 37, 5-7 (1980).
10. R.A. Athale, "Optical Matrix Algebraic Processors," in *Proc. 10th Int. Optical Computing Conf.*, IEEE, Cat. No. 83CH1880-4, April 1984, pp. 24-31.
11. R.A. Athale and W.C. Collins, "Optical Matrix-Matrix Multiplier Based on Outer Product Decomposition," *Appl. Opt.* 21, 2089-2090 (1982), and references therein.
12. See also papers in the Session on Optical Matrix Processing at the Topical Meeting in Optical Computing, March 18-20, Incline Village, NV, 1985.
13. C. Mead, "Potential and Limitations of VLSI," Topical Meeting in Optical Computing, March 18-20, Incline Village, NV, 1985.
14. B.K. Jenkins, A.A. Sawchuk, T.C. Strand, R. Forchheimer and B.H. Soffer, "Sequential Optical Logic Implementation," *Appl. Opt.* 23, 3455-3464 (1984).
15. B.K. Jenkins, P. Chavel, R. Forchheimer, A.A. Sawchuk and T.C. Strand, "Architecture Implementation of a Digital Optical Processor," *Appl. Opt.* 23, 3465-3474 (1984).



SC5502.AR

16. See, for example, R.A. Fisher, ed., Optical Phase Conjugation, Academic Press, NY (1983).
17. A.E.T. Chiou and P. Yeh, Opt. Lett. 11, 461 (1986).



SC5502.AR

## APPENDIX 5.1

### Optical Matrix-Vector Multiplication Through Four-Wave Mixing in Photorefractive Media



# Optical matrix-vector multiplication through four-wave mixing in photorefractive media

Pochi Yeh and Arthur E. T. Chiou

Rockwell International Science Center, Thousand Oaks, California 91360

Received September 3, 1986; accepted October 30, 1986

We propose and describe a new method of optical matrix-vector multiplication by using four-wave mixing in photorefractive media. Using a BaTiO<sub>3</sub> crystal, we have demonstrated such a parallel multiplication. The results are presented and discussed.

A large number of signal- and image-processing algorithms can be expressed in terms of matrix operations. The multiplication of two matrices is one of the most basic operations in matrix algebra. Optics, with its inherent parallelism, can offer great improvement in the speed of these operations. Optical processors for multiplying two matrices have been described in the literature.<sup>1-3</sup> Considerable work has also been reported on performing optical matrix-vector multiplication.<sup>3-5</sup> In this Letter, we describe a new method of performing matrix-vector multiplication by using optical four-wave mixing in nonlinear media. In addition, we also report the first experimental demonstration to our knowledge of such an optical matrix processor by using a photorefractive BaTiO<sub>3</sub> crystal.

Optical four-wave mixing has been a subject of considerable interest during the past several years. Much attention has been focused on wave-front-correction<sup>6-8</sup> and phase-conjugate interferometry.<sup>9,10</sup> In the area of signal processing, optical four-wave mixing has been used to perform spatial information processing,<sup>11</sup> image subtraction,<sup>12-15</sup> and logic operations.<sup>16</sup> However, little attention has been paid to the use of the inherently parallel multiplication nature of four-wave mixing for optical matrix multiplication. In this Letter we describe a new method of performing matrix-vector multiplication using four-wave mixing in nonlinear media.

In what follows, we briefly describe the basic principles of real-time matrix multiplication using optical four-wave mixing in nonlinear media. For the sake of convenience, we will limit ourselves to the case of square matrices, although extension to nonsquare matrices will be straightforward.

Referring to Fig. 1, we consider a scheme that is suitable for a matrix-vector multiplication. Here, as an example, let us consider a discrete case in which we need to carry out the multiplication of an  $N$ -element vector and an  $N \times N$  matrix. In this scheme, the vector is fanned out into  $N$  rows of identical vectors. These  $N \times N$  beamlets are directed to a nonlinear medium. The matrix, which also contains  $N \times N$  beamlets, is also directed to the medium in such a way that each beamlet of the matrix is counterpropagating in a direction relative to the corresponding beamlet of

the vector. Thus, in the medium, there are  $N \times N$  spatially separated regions, each of which is pumped by a pair of counterpropagating beamlets. Now a probing beam, which consists of  $N \times N$  beamlets, is directed into the medium in such a way that each probe beamlet will propagate through the corresponding intersection region, as shown in Fig. 1. The probe beam will be plane-wave beamlets propagating in parallel. All the beamlets in this probe beam are of equal intensity. As a result of the four-wave mixing, each probe beamlet will generate a phase-conjugated beamlet, which, within a proportional factor, can be written as  $M(i, j)a(j)$ . By using a cylindrical lens, a summation over  $j$  can be obtained. Thus we have

$$b(i) = \sum_j M(i, j) \times a(j), \quad (1)$$

where  $a(j)$  is the  $j$ th element of the vector  $\mathbf{a}$  and  $M(i, j)$  is the matrix element. Such a scheme for matrix-vector multiplication can also be used for matrix-matrix multiplication by decomposing a matrix into column vectors and then multiplying the matrix with each of the column vectors.

The probe beam can also simply be a uniform plane wave, without beamlets. The phase-conjugated beam will consist of  $N \times N$  beamlets, because only a matrix

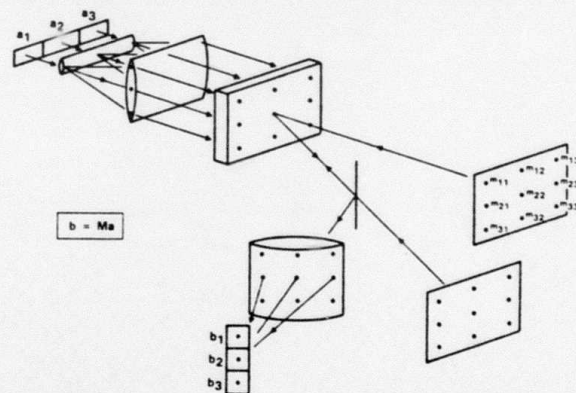


Fig. 1. Schematic drawing of the basic principle of optical matrix-vector multiplication through four-wave mixing in nonlinear media.

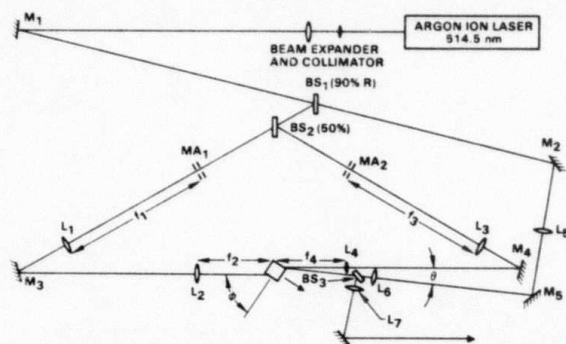


Fig. 2. Experimental setup used to demonstrate the optical matrix-vector multiplication.

of  $N \times N$  regions is pumped by counterpropagating beamlets. The matrix and the vector information can actually be carried on any two of the three incident beams in the four-wave mixing process.

The summation process can also be obtained without the external cylindrical lens by using a different scheme, described as follows. Consider a probe beam that consists of a column of  $N$  equal beamlets. The probe is incident into the nonlinear medium in such a way that each of the probe beamlets is made to propagate through a row of  $N$  intersection regions. The phase-conjugation process automatically performs the summation as well as the multiplication. The phase-conjugated beam is thus the product of the matrix-vector multiplication.

As a result of the nature of the four-wave mixing process in the medium, this new matrix-vector multiplier operates on the field amplitudes and thus can be used to handle matrices and vectors with complex elements. It is a coherent device rather than an incoherent one. This aspect is distinctly different from most of the earlier approaches, which are all incoherent. When the device is operated in the coherent mode, the phase of each beamlet must be maintained uniformly over the transverse dimension of the beamlet. In addition, such phases must also be maintained fixed in the summation process. If these phases are not uniform over the beamlets, the final step becomes an incoherent summation as a result of the spatial averaging. Under such circumstances, this matrix-vector multiplier operates on the intensities and thus handles only positive numbers.

The matrix-vector multiplication is demonstrated experimentally by using four-wave mixing in a photorefractive BaTiO<sub>3</sub> crystal.<sup>17</sup> The crystal is cut in such a way that the faces are all perpendicular to the principal axes. All the beams are polarized extraordinary in the  $xz$  plane and are incident onto the  $a$  faces of the crystal.

In our experiments, an Ar-ion laser beam at wavelength 514.5 nm with an output power of a few hundred milliwatts is used as the light source. The laser beam is expanded and collimated into a beam size of approximately 1 cm. Figure 2 shows our experimental setup. The expanded beam is then split into three beams by using beam splitters BS<sub>1</sub> and BS<sub>2</sub>. To dem-

onstrate the principle of operation, we chose the following matrix and vector:

$$M = \begin{bmatrix} 1 & 1 & 1 & 0 & 1 \\ 1 & 1 & 0 & 0 & 1 \\ 0 & 1 & 0 & 0 & 1 \\ 0 & 1 & 1 & 0 & 0 \\ 1 & 1 & 1 & 1 & 1 \end{bmatrix}, \quad \mathbf{a} = \begin{bmatrix} 1 \\ 0 \\ 1 \\ 1 \\ 1 \end{bmatrix}. \quad (2)$$

The matrix and the vector information is imprinted onto two of the beams by using transparencies (MA<sub>1</sub> and MA<sub>2</sub> in Fig. 2) that consist of circular dots. White circular dots represent the 1's, and the dark regions the 0's. Instead of using a cylindrical lens to fan out the vector into five identical rows as described earlier, we simply use a transparency of  $\mathbf{a}$  matrix that consists of five identical rows of (1 0 1 1 1). The incident matrices, corresponding to the matrix  $M$  and the vector  $\mathbf{a}$ , are shown in Figs. 3(a) and 3(b). Four lenses, L<sub>1</sub>, L<sub>2</sub>, L<sub>3</sub>, and L<sub>4</sub> (with focal lengths  $f_1 = f_3 = 0.5$  m and  $f_2 = f_4 = 0.2$  m) are used to image the transparencies MA<sub>1</sub> and MA<sub>2</sub> onto the center of the nonlinear crystal, where the diameter of each beamlet is 0.18 mm with a center-to-center distance of 0.51 mm. The size of the whole image inside the crystal is 2.2 mm  $\times$  2.2 mm. The uniform beam is also reduced (and collimated) to a diameter of 3.6 mm inside the crystal by lenses L<sub>5</sub> and L<sub>6</sub> (with focal lengths  $f_5 = 0.6$  m and  $f_6 = 0.25$  m, respectively). The angle  $\theta$  between the uniform beam and one of the pump beams is 11°. The two beams that carry the matrix and the vector information, respectively, are incident onto the opposite  $a$  faces of a photorefractive BaTiO<sub>3</sub> crystal. The incident angle  $\phi$  is approximately 20° with respect to the surface normal. As a result of the four-wave mixing, a phase-conjugated beam, consisting of a 5  $\times$  5 beamlet pattern, is generated and is shown in Fig. 3(c). A cylindrical lens is then used to perform the summation. The resulting product vector is shown in Fig. 3(d). By

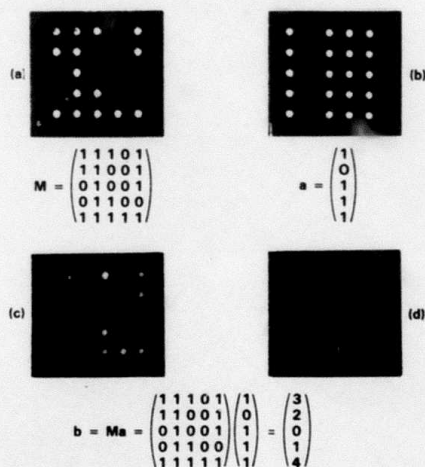


Fig. 3. Photographs showing the matrix and the vectors: (a) input matrix; (b) input vector, expanded into a matrix with five identical rows; (c) resultant phase-conjugate reflection matrix; (d) resultant vector of a matrix-vector multiplication after summation of (c) by a cylindrical lens.



measuring the intensity of the individual dots, we found that the product vector is (3 2 0 1 4), in good agreement with our prediction; in other words,

$$\mathbf{b} = \mathbf{M}\mathbf{a} = \begin{bmatrix} 1 & 1 & 1 & 0 & 1 & 1 \\ 1 & 1 & 0 & 0 & 1 & 0 \\ 0 & 1 & 0 & 0 & 1 & 1 \\ 0 & 1 & 1 & 0 & 0 & 1 \\ 1 & 1 & 1 & 1 & 1 & 1 \end{bmatrix} \begin{bmatrix} 3 \\ 2 \\ 0 \\ 1 \\ 4 \end{bmatrix} = \begin{bmatrix} 3 \\ 2 \\ 0 \\ 1 \\ 4 \end{bmatrix} \quad (3)$$

The intensities of the product vector elements are measured by integrating over the cross section of each beamlet. The experimental error is less than 5%. This small error is due to environmental perturbations and the slow response of the photorefractive crystal. Although our experiment demonstrates the operation for matrices and vectors with binary numbers (1, 0), this matrix-vector multiplier can also be operated in the analog mode to handle elements with gray levels. Such an analog operation in photorefractive crystals requires that the probe-beam intensity be weak so that the error due to the intensity denominator in the index modulation can be neglected. This material-related error disappears when the matrix and the vector contain only binary numbers (1, 0).

In conclusion, we have proposed and demonstrated a new method of matrix operation by using optical four-wave mixing in nonlinear media. In particular, we have demonstrated experimentally matrix-vector multiplication in a photorefractive BaTiO<sub>3</sub> crystal.

The authors acknowledge helpful discussions with M. D. Ewbank and M. Khoshnevisan (Rockwell International) and J. Neff (Defense Advanced Research Projects Agency).

## References

1. R. A. Athale, in *Proceedings of the Tenth International Optical Computing Conference*, Catalog No. 83CH1880-4 (Institute of Electrical and Electronics Engineers, New York, 1983), pp. 24-31.
2. R. A. Athale and W. C. Collins, *Appl. Opt.* **21**, 2089 (1982), and references therein.
3. See also papers in the session on optical matrix processing in *Digest of Topical Meeting on Optical Computing* (Optical Society of America, Washington, D.C., 1985), pp. TuD1-TuD7.
4. M. A. Monahan, K. Bromley, and R. P. Bocker, *Proc. IEEE* **65**, 121 (1977).
5. J. W. Goodman, A. R. Dias, and L. M. Woody, *Opt. Lett.* **2**, 1 (1978).
6. B. Ya. Zel'dovich, V. I. Popovichev, V. V. Ragul'skii, and F. S. Faizullov, *Sov. Phys. JETP* **15**, 109 (1972).
7. A. Yariv, *IEEE J. Quantum Electron.* **QE14**, 650 (1978).
8. C. R. Giuliano, *Phys. Today* **34**(4), 27 (1981).
9. M. Ewbank, P. Yeh, and M. Khoshnevisan, *Proc. Soc. Photo-Opt. Instrum. Eng.*, **464**, 2 (1984).
10. M. Ewbank, P. Yeh, M. Khoshnevisan, and J. Feinberg, *Opt. Lett.* **10**, 282 (1985).
11. See, e.g., J. O. White and A. Yariv, *Opt. Eng.* **21**, 224 (1982).
12. A. E. Chiou, P. Yeh, and M. Khoshnevisan, *Proc. Soc. Photo-Opt. Instrum. Eng.* **613**, 201 (1986).
13. S. Kwong, G. A. Rakuljic, V. Leyva and A. Yariv, *Proc. Soc. Photo-Opt. Instrum. Eng.* **613**, 36 (1986).
14. A. E. T. Chiou and P. Yeh, *Opt. Lett.* **11**, 306 (1986).
15. S. K. Kwong, G. A. Rakuljic, and A. Yariv, *Appl. Lett.* **48**, 201 (1986).
16. Y. Fainman, C. C. Guest and S. H. Lee, in *Digest of Topical Meeting on Optical Computing* (Optical Society of America, Washington, D.C., 1985), paper TuA5.
17. Sample of BaTiO<sub>3</sub> purchased from Sanders Associates, Nashua, N.H. 03061.



SC5502.AR

## APPENDIX 5.2

### Optical Matrix-Matrix Multiplication Using Multi-Color Four-Wave Mixing

## Optical Matrix-Matrix Multiplication using Multi-Color Four-Wave Mixing\*

Arthur E. Chiou, Monte Khoshnevisan and Pochi Yeh

Rockwell International Science Center

1049 Camino Dos Rios, Thousand Oaks, CA 91360

### SUMMARY

A new method for multiplying two  $N \times N$  matrices optically with  $N^3$  parallelism is described and demonstrated for the case of  $2 \times 2$  matrices in mixed binary modes. The basic idea is to decompose the original problem into  $N$  problems of matrix-vector multiplications which are carried out simultaneously (in parallel) using multi-color four-wave mixing. Recently, we have reported a new method of performing optical matrix-vector multiplication [1] using four-wave mixing in a nonlinear optical medium. For media which have significant nonlinear optical susceptibility over a range of wavelengths or at more than one wavelength (color), multi-color four-wave mixing [2] can be achieved; and several matrix-vector multiplications can be carried out simultaneously. We introduce a generic scheme which can extend such matrix-vector multiplications to matrix-matrix multiplication. Using a combination of angular and color multiplexing/demultiplexing techniques together with a multi-color four-wave mixing process, we show the multiplication of two matrices in parallel with time complexity of the order of  $N^3$ . Experimental results for the case of  $2 \times 2$  matrices using two-color four-wave mixing in a photorefractive barium titanate crystal are given. Some of the difficulties and the practical limit on the dimension ( $N$ ) of the matrix are discussed.

### REFERENCES

- [1] Pochi Yeh and Arthur Chiou, "Optical matrix-vector multiplication through four-wave mixing in photorefractive media," *Opt. Lett.* **12**, 138, (1986).
- [2] Tallis Y. Chang, D. L. Naylor, and R. W. Hellwarth, "Continuouswave Multi-Color Phase Conjugation," *Appl. Phys. B* **28**, 156 (1982).

\* This work has been supported by DARPA/AFOSR under Contract No. F49620-87-C-0015